Computational Materials Science 164 (2019) 133–138

Contents lists available at ScienceDirect

Computational Materials Science

journal homepage: www.elsevier.com/locate/commatsci

Study on collapse controlling of single-wall carbon nanotubes by helium storage

Penghua Ying[a,b,1], Yifan Zhao[a,1], Huifeng Tan[a,*]

[a] National Key Laboratory of Science and Technology for National Defence on Advanced Composites in Special Environments, Harbin Institute of Technology, Harbin 150001, PR China

[b] School of Science, Harbin Institute of Technology, Shenzhen 518055, PR China

ARTICLE INFO

Keywords:
Single-walled carbon nanotube
Helium storage
Configuration change
Collapse

ABSTRACT

In this paper, we propose a method to control the collapsed nanostructurings of single-walled carbon nanotubes (SWCNTs) by helium storage and the key mechanism is elaborated from the potential energy aspect. The molecular dynamics simulation shows that enough helium atoms could restore the collapsing configuration of (40, 40) carbon nanotubes back to the circular cross section. The length of the flat double carbon atoms layer in the dumbbell type structure and the diameter of nearly circular edges can be precisely altered by adjusting the helium atom numbers. Two key storage rates are introduced to classify the final nanostructures of (5*n*, 5*n*) SWCNTs. The relationship between helium numbers and the final configuration is investigated; the analysis method that introduces helium atoms into the cavity of SWCNTs can also be extended to other kinds of molecules.

1. Introduction

Carbon nanotubes (CNTs), having attracted massive interest in recent years, can be divided into zigzag, armchair and spiral ones according to the chirality. CNTs possess unique mechanical and physical properties compared with the traditional materials. It could be used as stretchable conductors, flexible strain sensors, field effect transistors and so on [1–3]. Generally, a natural equilibrium configuration of single-walled carbon nanotubes (SWCNTs) has a circular cross section. However, the parts of CNTs that subjected to hydrostatic pressure or compressive load will enter the van der Waals attraction zone and form a collapse configuration [4,5]. That is, the cross section of the nanostructures of CNTs are altered from circular to elliptical and polygonal, and then converted into completely collapsed peanut-like [6]. Cerqueira et al. [7] demonstrated that chirality has little effect on the collapse configuration via density functional theory. Aguiar et al. [8] theoretically analyzed the structural and phonon properties of bundled single- and double-walled carbon nanotubes (DWCNTs) and came to a conclusion that the difference of the collapsed configuration of SWCNTs mainly depends on the tube diameter. Xie et al. [9] and Yan et al. [10] found that the contact between CNTs and different solid surfaces or functional groups can also promote the collapse. As the collapse of CNTs tends to affect its physical properties [11–13], figuring out how to control the collapsing is a promising task.

Studies have demonstrated that graphene is an ideal molecular impervious membrane [14–17]; helium atoms cannot penetrate the wall of CNT curled by graphene [18,19]. These phenomenon enlighten us about novel methods to control the collapse of CNTs. The hollow CNTs could be filled with different kinds of molecules to realize various physical performances, owing to its molecular impervious property. Inert gases like helium [20,21], neon [22], argon [22–24], common gases including hydrogen [25] and carbon dioxide [26], and even water molecules [26–28] and fullerenes [20,29,30] all could be added into CNTs to control its properties. Through molecular mechanics and molecular dynamics simulations, Han et al. [31] found that the argon (Ar) and silicon (Si) atoms could effectively improve the radial elasticity and resistance of SWCNTs to high pressure, while the Cu atoms deteriorate the radial elasticity of SWCNTs. Cui et al. [26] studied the effect of filling the tube with carbon dioxide and water molecule by simulation. They found that the carbon dioxide provides mechanical support and increase the collapse pressure, while the water molecule inside could reduce the mechanical stability. As for the deformation of CNTs under hydrostatic pressure [32,33], Ling et al. [34] investigated the behavior of CNTs filled with fullerene under high pressure conditions, using molecular mechanics and molecular dynamics simulations.

The aforementioned studies have made progress in effects of guest

* Corresponding author.
E-mail address: tanhf@hit.edu.cn (H. Tan).
[1] These authors contributed equally: Penghua Ying, Yifan Zhao.

https://doi.org/10.1016/j.commatsci.2019.04.010
Received 21 November 2018; Received in revised form 18 March 2019; Accepted 8 April 2019

molecules on the transition pressure and radial elasticity of CNTs and corresponding optimization extent. This paper focuses on the relationship between the number of helium atoms and the stable nanostructure of SWCNTs after unloading. The molecular dynamics code LAMMPS [35] was used to model the (5*n*, 5*n*) CNTs. By inducing collapse and reaching a new equilibrium configuration, we found that enough helium atoms could restore the circular section of collapsing (40, 40) CNTs. In addition, a complementary simulation based on the final configurations was implemented under hydrostatic pressure to verify the robustness of the collapsing results. We discussed the mechanism of the collapse configuration change of CNTs from the potential energy aspect. Moreover, a fine-tuning effect on the dumbbell type CNTs is observed. Two critical storage rates, the configuration transformation storage rate (α_{tr}) and the minimum storage rate to restrain the collapse of CNTs (α_{re}), are obtained through simulations. According to the two critical storage rates, three different collapse nanostructures were defined.

2. Methods

The correct geometry of the collapsed CNTs is of great importance to obtain reliable results in the simulations. AIREBO [36] potential, continually used in the molecular simulations of CNTs, cannot produce the *ab initio* shapes of the closed edges [4]. Therefore, we select the Tersoff potential [37] for the simulations and add a Lennard-Jones interactions [38] between carbon atoms located in the opposite faces, which is the same as that adopted by Traian Dumitrică [39]. The Lennard-Jones parameters ($\varepsilon = 3.5$ *mev* and $\sigma = 0.34$ *nm*) used in this simulation are adjusted to describe a stress-free collapsing, which yields approximate results to those obtained through *ab initio* calculations and experiments [40]. The force field between the carbon and helium atoms and that between the helium atoms are also described by the Lennard-Jones potential. The parameters set in our simulation are $\varepsilon_{\text{He - He}} = 1.5008 \times 10^{-22}$ J, $\sigma_{\text{He - He}} = 2.633 \times 10^{-10}$ m, $\varepsilon_{\text{C - He}} = 2.6646 \times 10^{-22}$ J, and $\sigma_{\text{C - He}} = 3.191 \times 10^{-10}$ m [41].

The whole collapse process of the (5*n*, 5*n*) SWCNTs are carried out by the LAMMPS. The periodic boundary conditions are applied in the axial direction of the CNT, and the time step is 1 fs. The simulation process can be divided into three stages, as shown in Fig. 1. In the diffusion phase, a SWCNT model with a helium atom cluster is established and energy minimization is performed to make the configuration stable. In the loading phase, the SWCNTs are loaded with a small incremental displacement in vertical direction toward the center, with a speed of 0.08 A/ps, until the nanotubes completely collapse. In the unloading phase, the collapsing SWCNTs are unloaded and kept relaxed for about 200 ps. After that, the final structure of the CNTs with different helium numbers are obtained for further analysis.

For convenience, we use the storage rate α to represent the mass of helium atoms stored per unit mass of nanotubes. A single carbon atom is three times the mass of a single helium atom; hence helium storage rate in this paper can be described as follows:

$$\alpha = \frac{N_{\text{He}} m_{\text{He}}^{\text{atom}}}{N_{\text{C}} m_{\text{C}}^{\text{atom}}} = \frac{N_{\text{He}}}{3N_{\text{C}}}$$

where N_{He} is the number of helium atoms, and N_{C} the carbon atoms, in the simulation system; $m_{\text{He}}^{\text{atom}}$ is the mass of a single helium atom, and $m_{\text{C}}^{\text{atom}}$ the carbon atom.

3. Results and discussion

The molecular dynamics simulation is performed with 5 nm long (40, 40) SWCNTs. The system contains 3360 carbon atoms; the number of helium atoms are set as 600, 1640, and 2340, so the storage rates in this simulation are $\alpha_1 = 5.95\%$, $\alpha_2 = 16.27\%$, $\alpha_3 = 23.21\%$, respectively. The collapse processes are shown in Fig. 2. After 100 ps, as the storage rate increases, the helium atom layers gradually form a double or a multi-layer structure. The distance between helium atoms and SWCNT wall represents the equilibrium distance determined by van der Waals interaction. When 100 ps < t < 400 ps, the upper and lower regions of the nanotubes are simultaneously loaded with small vertical incremental displacements toward the center. The distributions of helium atoms under different storage rates from 230 ps to 360 ps are in line with those observed by Shanavas and Sharma, *i.e.*, the diffusion of argon inside the CNTs under no-pressure condition [42]. When$t$ = 400 ps, the loading is stopped, the CNTs in three simulation systems all show a peanut type configuration, with two semi-elliptical sides connected by a cosine function curve in the middle part [5]. The carbon atoms in the deformation zone do not directly contact with each other, and the part of the cosine function curve is separated by layers of helium atoms. Between 400 ps and 600 ps, the CNTs are in unloading and relaxing.

During the relaxation process which containing 200,000 steps, the final configurations of CNTs are altered, as shown in Fig. 2. The model with a storage rate of 5.95% changed from peanut type to dumbbell type. Here we define the length of the flat double carbon atoms layer especially in the dumbbell type as l_{flat}, details of which are discussed in the following paragraph. The final configuration of the model with 16.27% storage rate is maintained peanut-like, while the cross section of the nanotube with the 23.21% storage rate is noticeably restored to be circular. Actually the final configurations have been stable after 420 ps.

The fact that the number of helium atoms influences the final configuration of CNTs can be explained in terms of the energy of the structure. The changes in the energy value and the corresponding

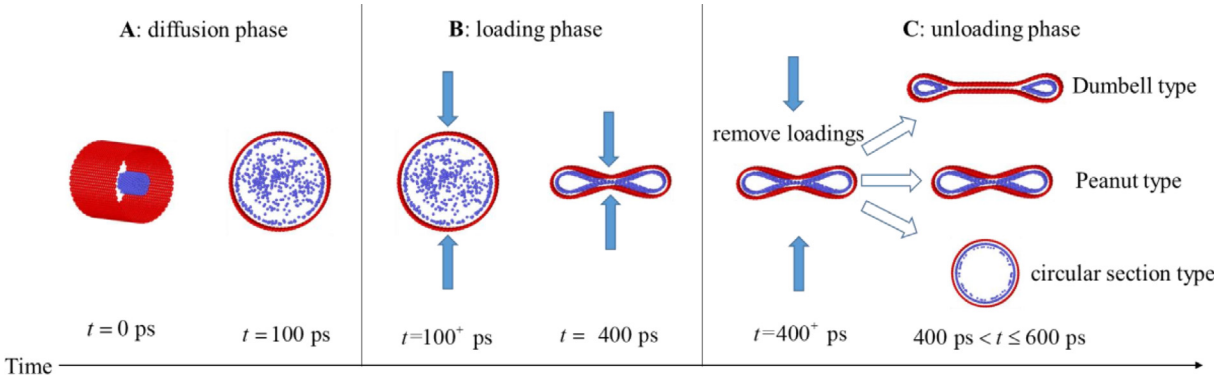

Fig. 1. In stage A, the NVT ensemble is applied to set the temperatures of SWCNT and helium atoms to be 0.001 K and 100 K, respectively. The total simulation time for this stage is 100 ps. In stage B, The temperature of helium atoms is set to be 10 K to get rid of the thermal disturbance[31]. The running time for this stage is 300 ps. In stage C, the SWCNTs are unloaded at 400 ps. After keeping relaxed for about 200 ps, the equilibrium configurations are dumbbell type, peanut type and circular section type.

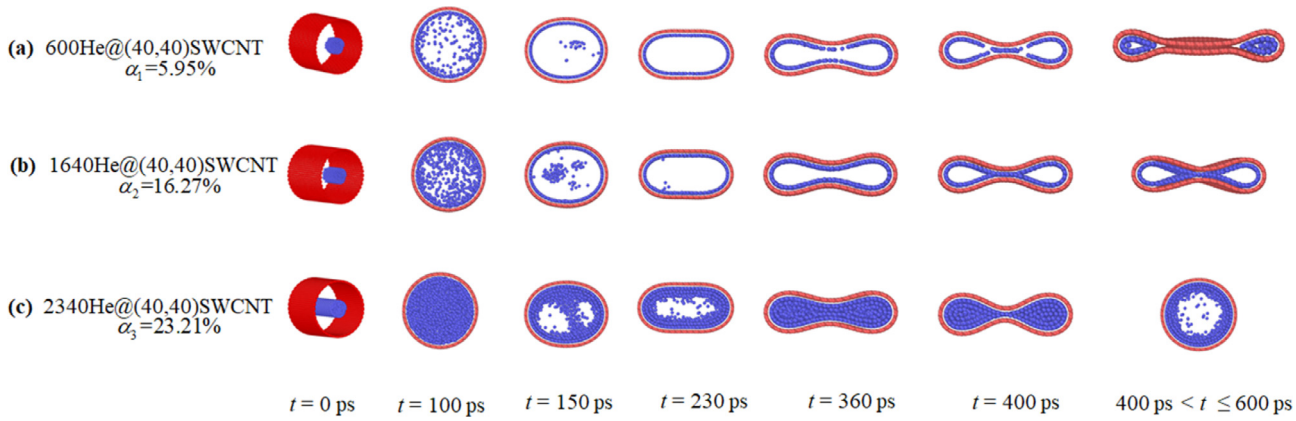

Fig. 2. Diagram of collapse process of (40, 40) SWCNTs with three different helium storage rates, in which the red atoms represent carbon atoms and the blue ones represent helium atoms. Initial states of SWCNTs are given at 0 ps, between 100 ps and 400 ps is the loading process, between 400 ps and 600 ps is the relaxation process. (a) α_1 = 5.95% dumbbell type configuration, (b) α_2 = 16.27% peanut type configuration, (c) α_3 = 23.21% circular section type configuration.

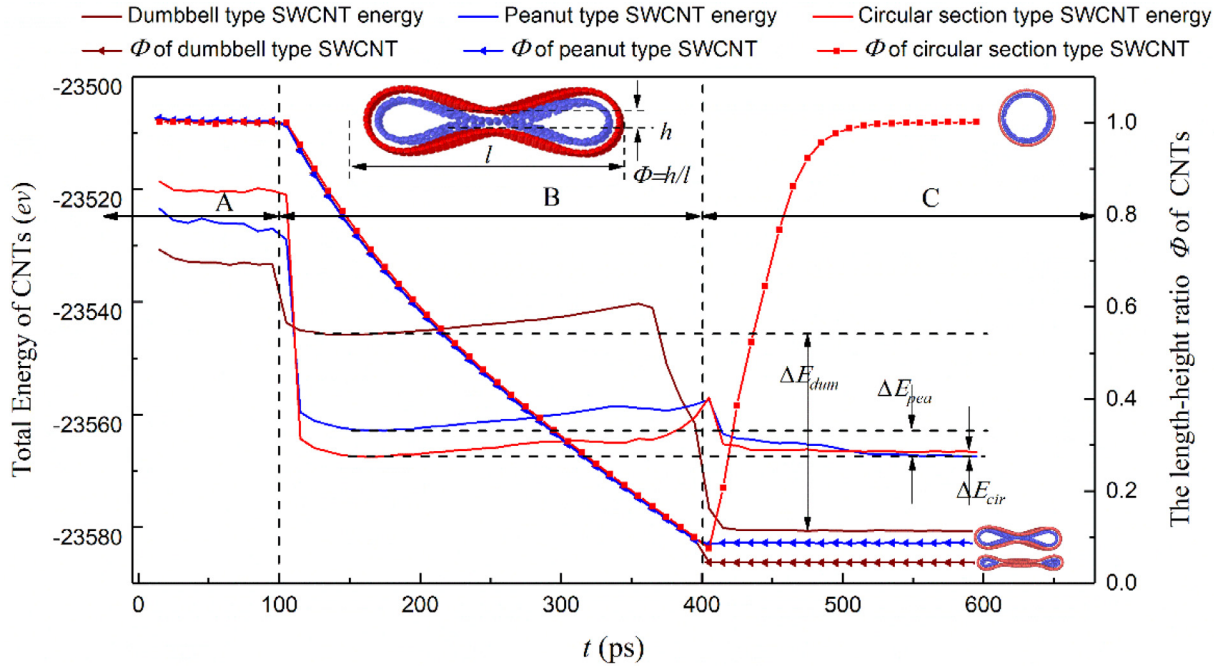

Fig. 3. Variation of total energy and length-height ratio Φ of (40, 40) SWCNTs in three different collapse configurations. The stages A, B, and C represent the helium atoms diffusion phase, the loading phase, the unloading and stabilization phase, respectively.

extent to which configurations of the three SWCNT models transform are plotted in Fig. 3. Here we introduce the length-height ratio, Φ, as a variable used to quantify the deformation extent; it is defined as the ratio of the height of the gap at the narrow region (h) to the distance between the left and right ends (l) of the SWCNTs. In the stage A, Φ of the three storage rates is 1 or approximately equals to 1. The total energy of the structure increases with the increase of the storage rate, mainly due to the fact that the more the helium atoms, the larger the van der Waals energy between the helium atoms. In the stage B, Φ values show a consistent downward trend, while the energy firstly decreases sharply and then increases gently. In this process, the atomic temperature of helium is reduced from 100 K to 10 K and the helium atoms gradually form a complete inner wall. As the simulation continues, the further deformation of CNTs and the gentle rise of energy indicate the reinforced repulsive force between the helium and carbon atoms. In the stage C, the three configurations change dramatically after unloading. The Φ of the nanotube with α_3 = 23.21% recovers to 1 again, to 0.088 for the nanotube with α_2 = 16.27%, and to 0.045 for the nanotube with α_1 = 5.95%. Three models can be sorted according to the magnitudes of their energies: the SWCNT which has final configuration of dumbbell type has the lowest energy, followed by the circular section type and the peanut type has the highest energy. Therefore, a conclusion can be drawn that the number of helium atoms affects van der Waals energy; this energy is exactly the key factor that affects the stability of CNTs.

According to Fig. 3, we find that the dumbbell type system has lower energy than peanut type system, because the narrow part of a peanut type is only maintained by a few carbon atoms under van der Waals force. These carbon atoms have large freedom to slip, making the system unstable. The variables ΔE_{dum}, ΔE_{pea} and ΔE_{cir} in Fig. 3 denote different values between the minimum energy and the final energy of dumbbell type, peanut type and circular section type system, respectively. These relations, $\Delta E_{dum} > 0$, $\Delta E_{cir} \approx 0$, $\Delta E_{pea} > 0$, mean that the three type are all in the steady state, and the dumbbell type is the most stable configuration.

During the simulation, a fine-tuning effect of helium numbers on the collapsing SWCNTs is found, as shown in Fig. 4. When the storage rate is lower than 11.09%, the final configuration of CNTs is dumbbell type

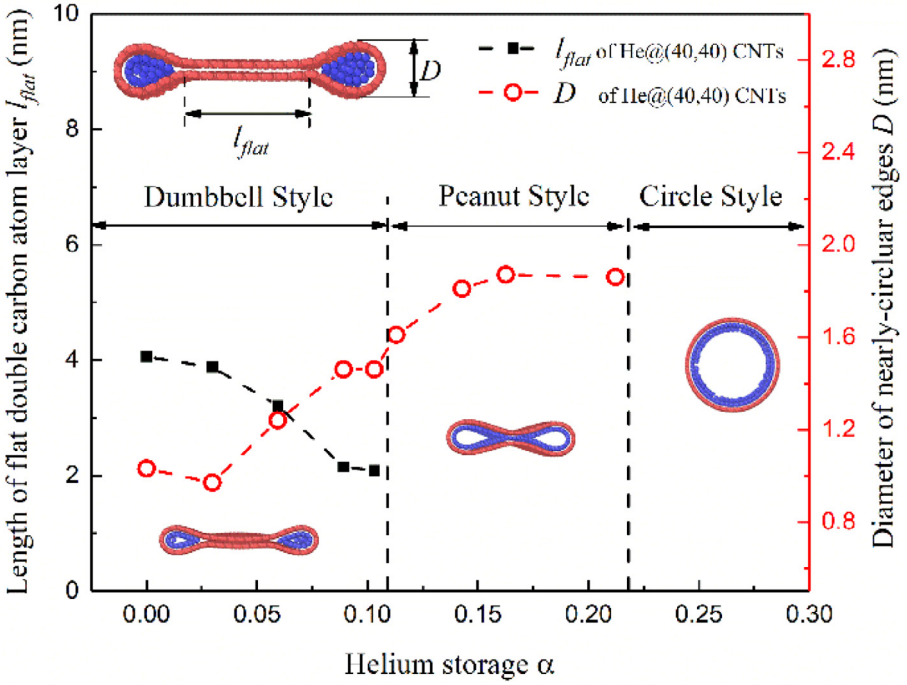

Fig. 4. The variation of length of the flat double carbon atoms layer, l_{flat}, and the diameter of the circular edges, D, with respect to the helium atoms. l_{flat} is disappeared while the peanut type occurs, and D reaches the maximum value, 1.86 nm, with the approximate linear relationship.

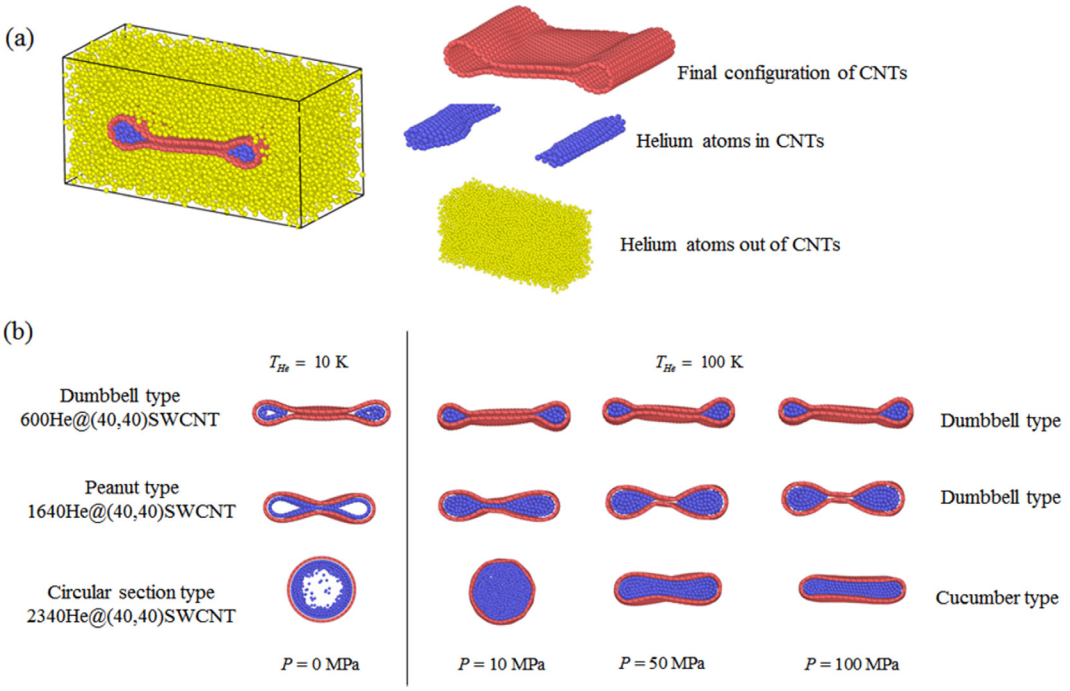

Fig.5. (a) Diagram of a complementary simulation of the CNT with final collapsing configuration under hydrostatic pressure. The Berendsen barostat is used to reset the pressure of the helium atoms out of CNTs, which rescales the volume and the coordinates of helium atoms out of CNTs every timestep [44]. The NVT ensemble is applied to set the temperatures of SWCNT and helium atoms to be 0.001 K and 100 K, respectively. The starting and ending pressures in the simulation are 10 MPa and 100 MPa, respectively. The periodic boundary conditions are applied in three directions. (b) Variation of three final configurations of (40, 40) CNTs under hydrostatic pressure. The final configurations altered are peanut type and circular section type, which transformed into dumbbell type and cucumber section type.

with a relatively long flat double carbon atoms layer. As the number of helium increases, the semi-elliptical areas on both sides become larger. The diameter of the nearly circular edges, D, increases approximately linearly with respect to the helium atoms; simultaneously, the l_{flat} decreases linearly. When $11.09\% \leq \alpha < 22.22\%$, the peanut type occurs because of the instantaneous disappearance of l_{flat}. The diameter of nearly circular edges, D, increases with the storage rate until it reaches a maximum value of about 1.86 nm. When $a \geq 22.22\%$, the l_{flat} and D are disappeared, which means the storage rate completely suppresses the collapse.

In fact, collapsed nanotubes are stacked in bundles [39,43] instead of isolated. To make the simulation reveal the actual case better, the

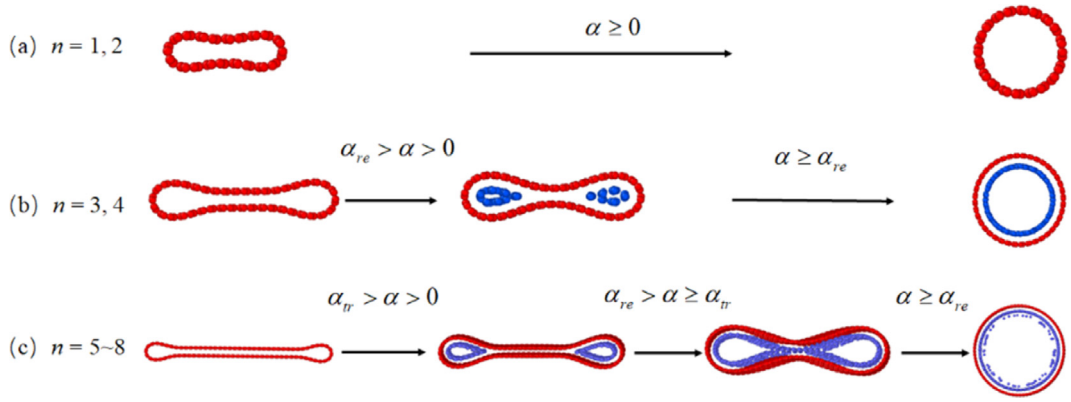

Fig. 6. The final configuration type of (5*n*, 5*n*) SWCNTs collapsed with different storage rates.

influence of interaction between neighbor tubes should be taken into account. The interaction between CNTs induced by van der Waals force can be described as hydrostatic pressure. As illustrated in Fig. 5(a), the simulation is implemented based on the CNTs with different final configurations obtained in the above analysis, and the results are shown in Fig. 5(b). The change of temperature of helium atoms in CNTs guarantees the uniform distribution of helium atoms in CNTs; the external pressure is generated by helium atoms, varying from 10 MPa to 100 MPa. The results show that the structure of dumbbell type CNTs remained unchanged during the whole simulation process. However, when the pressure reaches 50 MPa, the helium atoms in the peanut-shaped waist part move to the semi-elliptical area on both sides, the peanut type CNT changes into a dumbbell type one and remains stable until the simulation ending. Circular section type CNT undergoes the greatest deformation among three types of CNTs. Under the pressure of 50 MPa, the circular section transforms into a cucumber section with a flat middle and a semicircle on both sides. These results help to verify the reliability of our conclusion, that is, the collapsed CNTs are all in a stable state, and different storage rates do affect the types of section shape of the final configuration.

Two key storage rates are introduced to divide the CNTs into three final configurations. The α_{tr} indicates a critical storage rate below which the final configuration is dumbbell type, when the storage rate of helium atoms exceed α_{tr}, the final configuration transforms to peanut type. And the α_{re} represents a minimum storage rate over which the helium can restrain collapse. According to the results, for the (40, 40) nanotubes simulated in this paper, α_{tr} is 11.09\% and α_{re} is 22.22%.

The entire collapse processes of (5*n*, 5*n*) SWCNTs (n = 3–8, n is an integer) filled with different numbers of helium are modeled to give more intensive insights on such structure. The configuration changes are shown in Fig. 6. When $n = 1$ or 2, the circular section of the SWCNTs remains stable no matter whether helium exists or not, that is, the collapse configuration always returns to the circular section. This is consistent with existing research results [5]. When $n = 3$ or 4, the final configurations after collapse are peanut type. Due to the limitation of the nanotubes radius, there is no flat double carbon atoms layer in the final configuration, so the outer contour is still the peanut-like configuration with two semi-elliptical sides linked by cosine curve. As the storage rate increases beyond α_{re}, the final configuration returns to a circular section type. When n = 5–8, different values of α leads to three kinds of final configurations. The dumbbell type appears in the case of the storage rate lower than α_{tr}, the peanut type appears in the case of the storage rate between α_{tr} and α_{re}, and when the storage rate is higher than α_{re}, the configuration will return to the circular section type.

4. Conclusions

Suffering external pressure, different level of collapse occurs on SWCNTs when its diameter exceeds a certain value. In this paper, the results show that filling helium has an effect on the final configuration of collapse SWCNTs. As for the (40, 40) SWCNTs, a small storage rate can result in a dumbbell type configuration. When the storage rate increases, the final configuration will transform to a peanut type and even to the one with a fully restored circular section. It is safe to state that all the three configurations are steady, while the dumbbell type is the most stable configuration. When adjusting the storage rate in a certain range, the length of the flat double carbon atoms layer of dumbbell type changes approximately linearly. The diameter of nearly circular edges increases with respect to the storage rate until it reaches a maximum value. The results shown in this paper may pave the way for further study on how to control collapse of SWCNTs by filling guest particles.

CRediT authorship contribution statement

Penghua Ying: Methodology, Investigation, Formal analysis, Writing - review & editing. **Yifan Zhao:** Investigation, Formal analysis, Writing - original draft, Writing - review & editing. **Huifeng Tan:** Conceptualization, Supervision, Validation.

Acknowledgements

The authors would thank to the School of Astronautics Harbin Institute of Technology for providing the computational facilities for this research. The authors thank associate professor Zhang Jing of Harbin Institute of Technology for stimulating discussion.

Conflicts of interest

This research did not receive any specific grant from funding agencies in the public, commercial, or not-for-profit sectors.

Appendix A. Supplementary data

Supplementary data to this article can be found online at https://doi.org/10.1016/j.commatsci.2019.04.010.

References

[1] S. Yao, Y. Zhu, Nanomaterial-enabled stretchable conductors: strategies, materials and devices, Adv. Mater. 27 (9) (2015) 1480–1511.
[2] Y. Wang, R. Yang, Z. Shi, et al., Super-elastic graphene ripples for flexible strain sensors, ACS Nano 5 (5) (2011) 3645–3650.
[3] B.J. Kim, H. Jang, S.-K. Lee, et al., High-performance flexible graphene field effect transistors with ion gel gate dielectrics, Nano Lett. 10 (9) (2010) 3464–3466.
[4] G.H. Gao, W.A. Goddard, T. Cagin, Energetics, structure, mechanical and vibrational properties of single-walled carbon nanotubes, Nanotechnology 9 (3) (1998) 184–191.
[5] W. Lu, T.W. Chou, B.S. Kim, Radial deformation and its related energy variations of single-walled carbon nanotubes, Phys. Rev. B: Condens. Matter 83 (13) (2011) 059901.

[6] J. Zang, A. Treibergs, Y. Han, et al., Geometric constant defining shape transitions of carbon nanotubes under pressure. Phys. Rev. Lett. (2004) 92(10).
[7] T.F.T. Cerqueira, S. Botti, A. San-Miguel, et al., Density-functional tight-binding study of the collapse of carbon nanotubes under hydrostatic pressure, Carbon 69 (2) (2014) 355–360.
[8] A.L. Aguiar, R.B. Capaz, A.G.S. Filho, et al., Structural and phonon properties of bundled single- and double-wall carbon nanotubes under pressure, J. Phys. Chem. C 116 (42) (2012) 22637–22645.
[9] J. Xie, Q. Xue, H. Chen, et al., Influence of solid surface and functional group on the collapse of carbon nanotubes, J. Phys. Chem. C 114 (5) (2014) 2100–2107.
[10] K.Y. Yan, Q.Z. Xue, Q.B. Zheng, et al., Radial collapse of single-walled carbon nanotubes induced by the Cu2O surface, J. Phys. Chem. C 113 (113) (2014) 3120–3126.
[11] J.Q. Lu, J. Wu, W.H. Duan, et al., Metal-to-semiconductor transition in squashed armchair carbon nanotubes, Phys. Rev. Lett. 90 (15660115) (2003) 156601.
[12] R. Martel, T. Schmidt, H.R. Shea, et al., Single- and multi-wall carbon nanotube field-effect transistors, Appl. Phys. Lett. 73 (17) (1998) 2447–2449.
[13] C.J. Park, Y.H. Kim, K.J. Chang, Band-gap modification by radial deformation in carbon nanotubes, Physical Review B. 60 (15) (1999) 10656–10659.
[14] V. Berry, Impermeability of graphene and its applications, Carbon 62 (10) (2013) 1–10.
[15] R.R. Nair, A.K. Geim, Unimpeded permeation of water through helium-leak-tight graphene-based membranes, Science 335 (6067) (2012) 442.
[16] H.W. Kim, H.W. Yoon, S.M. Yoon, et al., Selective gas transport through few-layered graphene and graphene oxide membranes, Science 342 (6154) (2013) 91–95.
[17] K.C. Kemp, H. Seema, M. Saleh, et al., Environmental applications using graphene composites: water remediation and gas adsorption, Nanoscale 5 (8) (2013) 3149.
[18] J.S. Bunch, S.S. Verbridge, J.S. Alden, et al., Impermeable atomic membranes from graphene sheets, Nano Lett. 8 (8) (2008) 2458.
[19] O. Leenaerts, B. Partoens, F.M. Peeters, Graphene: a perfect nanoballoon, Appl. Phys. Lett. 93 (19) (2008) 183.
[20] R.E. Tuzun, D.W. Noid, B.G. Sumpter, et al., Dynamics of He/C60 flow inside carbon nanotubes, Nanotechnology 8 (8) (1997) 112.
[21] M.K. Agusta, I. Prasetiyo, A.G. Saputro, et al., First-principles molecular dynamics study on helium-filled carbon nanotube, J Phys Conf Series (2016) 012081.
[22] David M. Ackerman, Anastasios I. Skoulidas, David S. Sholl, et al., Diffusivities of Ar and Ne in carbon nanotubes, Mol. Simul. 29 (10–11) (2003) 677–684.
[23] Y.C. Liu, J.D. Moore, T.J. Roussel, et al., Dual diffusion mechanism of argon confined in single-walled carbon nanotube bundles, Phys. Chem. Chem. Phys. 12 (25) (2010) 6632–6640.
[24] J. Cannon, D. Kim, O. Hess, The initial flow dynamics of light atoms through carbon nanotubes, Fluid Dyn. Res. 43 (2) (2011) 025507.
[25] Martynková GS, Rozumová L, Hundáková M. Molecular modeling of hydrogen and selected types of CNT's interactions, Nanocon; 2013.
[26] W. Cui, T.F. Cerqueira, S. Botti, et al., Nanostructured water and carbon dioxide inside collapsing carbon nanotubes at high pressure. PCCP 18 (29) (2016).
[27] A.C. Torres-Dias, S. Cambré, W. Wenseleers, et al., Chirality-dependent mechanical response of empty and water-filled single-wall carbon nanotubes at high pressure, Carbon 95 (2015) 442–451.
[28] G. Algarasiller, O. Lehtinen, F.C. Wang, et al., Square ice in graphene nanocapillaries. Nature 519 (7544) (2015) 443.
[29] C. Caillier, D. Machon, A. San-Miguel, et al., Probing high-pressure properties of single-wall carbon nanotubes through fullerene encapsulation, Phys. Rev. B 77 (12) (2008).
[30] M. Chorro, J. Cambedouzou, A. Iwasiewiczwabnig, et al., Discriminated structural behaviour of C60 and C70 peapods under extreme conditions, EPL 79 (79) (2007) 56003.
[31] Z.D. Han, C.C. Ling, Q.K. Guo, et al., Influence of filling atoms on radial collapse and elasticity of carbon nanotubes under hydrostatic pressure, Sci. Bull. 60 (17) (2015) 1509.
[32] N.M. Pugno, The design of self-collapsed super-strong nanotube bundles, J. Mech. Phys. Solids 58 (9) (2010) 1397–1410.
[33] X. Yang, G. Wu, J. Dong, Structural transformations of double-walled carbon nanotube bundle under hydrostatic pressure, Appl. Phys. Lett. 89 (11) (2006) 095506.
[34] C. Ling, Q. Xue, D. Xia, et al., Fullerene filling modulates carbon nanotube radial elasticity and resistance to high pressure, RSC Adv. 4 (3) (2013) 1107–1115.
[35] S. Plimpton, Fast parallel algorithms for short-range molecular dynamics, J. Comput. Phys. 117 (1) (1995) 1–19.
[36] S.J. Stuart, A.B. Tutein, J.A. Harrison, A reactive potential for hydrocarbons with intermolecular interactions, J. Chem. Phys. 112 (14) (2000) 6472–6486.
[37] J. Tersoff, Empirical interatomic potential for carbon, with applications to amorphous carbon, Phys. Rev. Lett. 61 (1988) 2879.
[38] J.E. Jones, On the determination of molecular fields. II. From the equation of state of a gas, Proc. R. Soc. London 106 (738) (1924) 463–477.
[39] J. Al-Ghalith, et al., Collapsed carbon nanotubes as building blocks for high-performance thermal materials, Phys. Rev. Mater. 1 (5) (2017).
[40] J.A. Elliott, J.K.W. Sandler, A.H. Windle, R.J. Young, M.S.P. Shaffer, Collapse of singlewall carbon nanotubes is diameter dependent, Phys. Rev. Lett. 92 (2004) 095501.
[41] I. Hanasaki, A. Nakatani, H. Kitagawa, Molecular dynamics study of Ar flow and He flow inside carbon nanotube junction as a molecular nozzle and diffuser, Sci. Technol. Adv. Mater. 5 (1) (2004) 107–113.
[42] K.V. Shanavas, S.M. Sharma, Molecular dynamics simulations of phase transitions in argon-filled single-walled carbon nanotube bundles under high pressure, Phys. Rev. B: Condens. Matter 79 (15) (2009) 897–899.
[43] R.D. Downes, et al., Geometrically constrained self-assembly and crystal packing of flattened and aligned carbon nanotubes, Carbon 93 (2015) 953–966.
[44] H.J.C. Berendsen, J.P.M. Postma, W.F. van Gunsteren, A. DiNola, J.R. Haak, Molecular dynamics with coupling to an external bath, J. Chem. Phys. 81 (1984) 3684.